Influence of temperature on the reduction kinetics of Zn2+ at a mercury electrode

ARTICLE *in* JOURNAL OF ELECTROANALYTICAL CHEMISTRY · APRIL 2003

Impact Factor: 2.73 · DOI: 10.1016/S0022-0728(02)01432-8

Available online at www.sciencedirect.com
SCIENCE DIRECT®
Journal of Electroanalytical Chemistry 552 (2003) 247–259
Journal of Electroanalytical Chemistry
www.elsevier.com/locate/jelechem

Influence of temperature on the reduction kinetics of Zn^{2+} at a mercury electrode

G. López-Pérez, R. Andreu *, D. González-Arjona, J.J. Calvente, M. Molero

Department of Physical Chemistry, University of Seville, Seville E-41012, Spain

Received 26 August 2002; received in revised form 28 October 2002; accepted 22 November 2002

Dedicated to Professor B.B. Damaskin on the occasion of his 70th birthday and in honor of his contributions to electrochemistry

Abstract

The reduction of Zn^{2+} at a mercury electrode has been studied by the a.c. impedance technique in the 263–318 K temperature range. Kinetic data have been analyzed in terms of a mechanism consisting of two consecutive charge transfer steps. The apparent activation enthalpies and charge transfer coefficients of both steps are found to be temperature independent. Differential capacity curves and potentials of zero charge of the $NaClO_4$ supporting electrolyte solutions were measured at each temperature of interest. Double layer effects on the Zn^{2+} reduction rate constants were analyzed within the framework of the unequal distances of closest approach theory, and the corrected rate constants were found to be independent of supporting electrolyte concentration when allowance for changes in the Zn^{2+} activity coefficient was made. The implications of the activation parameter values on the nature of the rate determining steps are also discussed.

Keywords: a.c. impedance; Activation energy; Heterogeneous electron transfer rate constant; Double layer; Interfacial structure; Temperature

1. Introduction

Amalgam forming electrode reactions have been extensively studied in the literature [1,2], but some fundamental aspects of their mechanism are still not well understood. Plots of the logarithm of the forward rate constant as a function of the applied potential are often non-linear [3–10], displaying a curvature which cannot simply be explained by either double layer effects or the quadratic dependence on potential predicted by Marcus theory. Therefore, it seems that the mechanism of these electrochemical reactions is complex, and that the nature of the rate determining step changes with potential. Cationic deposition can then be envisaged as a series of elementary steps, characterized by a distinct dependence on potential, such as electron transfer, chemical transformation (e.g. ligand exchange or dehydration), ion transfer or partial charge transfer [11–13].

The reduction of Zn^{2+} offers some practical advantages in the exploration of the mechanism of amalgam forming reactions, since it exhibits rather slow charge transfer kinetics and it proceeds at potentials far negative from the potential of zero charge, thus allowing the acquisition of kinetic information over a wide potential range and in the absence of specific adsorption. The variation of the logarithm of the rate constant with potential was originally explained in terms of two consecutive electron transfer processes [14–16], without considering explicitly any displacement of charged species through the double layer. However, an alternative interpretation was offered by Fawcett [17], who showed that the same dependence of the rate constant on potential was predicted by a mechanism consisting of consecutive ion transfer steps from a site near the outer Helmholtz plane to a site in the inner layer, and then from the inner layer to a site where the metal ion is adsorbed. More recently, Pecina and Schmickler [18] have studied the deposition of Zn^{2+} from an aqueous solution by molecular dynamics. Their results indicate that the minimum energy reaction pathway involves the

* Corresponding author. Tel.: +34-95-4557175; fax: +34-95-4557174.
E-mail address: fondacab@us.es (R. Andreu).

0022-0728/02/$ - see front matter
doi:10.1016/S0022-0728(02)01432-8

presence of a less hydrated Zn^+ intermediate, whose distance of closest approach to the electrode is smaller than that of Zn^{2+}. Therefore, it now seems likely that the reaction mechanism includes not only electron transfer and dehydration steps [4], but also ion transfer steps [17].

The study of the double layer effects resulting from changes in the nature of the electrolyte ions has been proposed as an experimental strategy aimed at locating the position of the rate determining step within the double layer [19]. In a previous report [20], a consistent correction of double layer effects on the Zn^{2+} reduction rate, in the presence of $LiClO_4$, $NaClO_4$, $Mg(ClO_4)_2$ and $Al(ClO_4)_3$, has been achieved by assuming that two consecutive charge transfer steps are rate determining, and that the first charge transfer step was an electron exchange taking place at the plane of closest approach of Zn^{2+}, i.e. at 0.39 nm from the electrode surface.

The present work intends to gain some additional information on the mechanism of Zn^{2+} reduction at mercury through the analysis of the variation of its rate constant with temperature, since theoretical simulations [21] indicate that the activation energy and charge transfer coefficient associated with a rate determining ion transfer step should decrease with increasing temperature.

2. Experimental

Measurements were carried out in a three-electrode cell. A saturated sodium chloride calomel electrode (SSCE), connected to the cell via a salt bridge containing the cell solution, was used as the reference electrode, and was kept at room temperature (24 ± 2 °C). A platinum foil of high surface area (≈ 1 cm^2) was employed as the counter electrode. The working electrode was a static mercury drop electrode, EG&G PAR model 303A, modified to improve the reproducibility of the drop area [22]. Mercury was purified by treatment with dilute nitric acid and mercurous nitrate, and subsequently distilled three times under vacuum.

Sodium perchlorate solutions were made up from Merck analytical grade reagent and water purified by a Millipore Milli-Q system. The $Zn(ClO_4)_2$ solutions were prepared by dissolving ZnO in a small excess of perchloric acid, making the final solution 10^{-3} M in H^+ to avoid hydrolysis of Zn^{2+}. The $Zn(ClO_4)_2$ concentration in the cell was varied within the 6–30 mM range, in order to improve the experimental accuracy at each temperature.

Oxygen was removed by bubbling nitrogen, which had been pre-saturated in the cell solution. The temperature of each experiment was controlled within ± 0.1 K with a Haake D8.G circulator thermostat, using an ethanol + water mixture as the heat exchanger fluid in the 263–318 K temperature range. The lowest temperature for each solution was chosen ca. 5° above its freezing point.

Impedance measurements were carried out with an automated acquisition system, which has been described previously [23]. It is based upon the Solartron 1286 FRA and the Solartron 1256 electrochemical interface, allowing simultaneous recording of the d.c. and a.c. responses of the cell. Cell impedances were measured at 12 frequencies in the 70–2020 Hz range. The ohmic resistance was determined at 10 kHz outside the faradaic region, and d.c. potentials were corrected for ohmic drops when necessary. Potentials of zero charge were determined by the streaming electrode technique [24]. Differential capacity curves of $NaClO_4$ solutions were measured at 1020 Hz.

3. Results

3.1. General behavior

The influence of temperature on the electrochemical discharge of Zn^{2+} can be easily visualized in the set of polarograms depicted in Fig. 1. Thus, a decrease of temperature produces lower diffusion limited currents, a shift of the wave towards more negative potentials, and smaller slopes along the rising part of the polarograms. Each of these observations is related to the temperature dependence of a different kinetic or thermodynamic parameter, which we shall now consider in some detail.

Changes in the limiting current values (I_{lim}) with temperature can be described in terms of the thermal activation of the Zn^{2+} diffusion process in solution, so

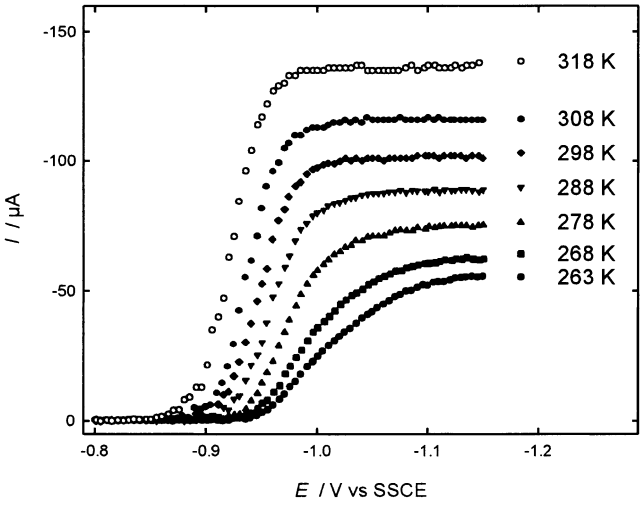

Fig. 1. Influence of temperature on normal pulse polarograms of Zn^{2+} in the presence of 4 M $NaClO_4$ supporting electrolyte. Temperature is indicated for each curve. Electrode area: 0.0269 cm^2, Zn^{2+} concentration: 0.02 M. Current was recorded 4 s after application of the potential pulse on a new mercury drop.

that:

$$D_O = A_D \exp\left(\frac{-E_D^a}{RT}\right) \quad (1)$$

where D_O is the diffusion coefficient of Zn^{2+}, and A_D and E_D^a stand for the pre-exponential factor and the activation energy for diffusion, respectively. Values of D_O were obtained from Koutecky's equation for the limiting current. The linearity of the log D_O vs T^{-1} plots (Fig. 2a) confirms the adequacy of Eq. (1). From the slopes, $E_D^a = 20.5 \pm 0.5$ kJ mol^{-1} is obtained, which turns out to be independent of the $NaClO_4$ concentration in solution. This result agrees with $E_D^a = 21.1$ kJ mol^{-1} reported for Cr^{2+} [25], while trivalent cations, such as Cr^{3+}, show a higher activation energy (23.3 kJ mol^{-1}) in aqueous media, as expected from their higher hydration energies and radii. Values of the diffusion coefficients of zinc in mercury (D_R) at different temperatures were taken from the literature [26], and they show a weaker temperature dependence, corresponding to $E_D^a = 7$ kJ mol^{-1}.

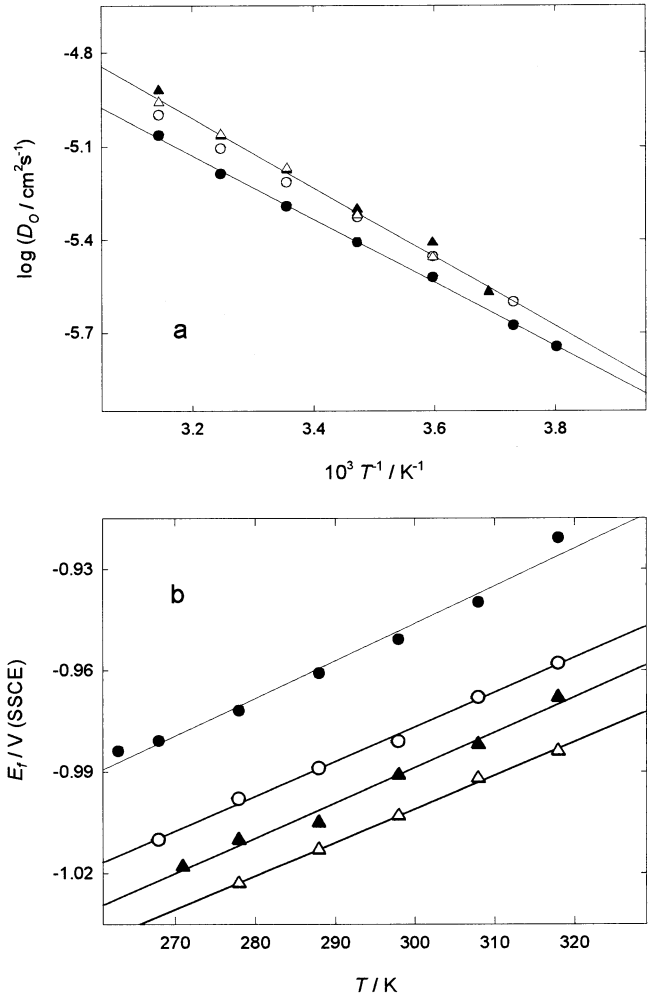

Fig. 2. (a) Arrhenius plot of the logarithm of the Zn^{2+} diffusion coefficient, and (b) variation with temperature of the formal potential of Zn^{2+} reduction measured against an isothermal reference electrode. Symbols correspond to the following sodium perchlorate concentrations: (△) 0.5 M, (▲) 1 M, (○) 2 M and (●) 4 M.

The displacement of the waves along the potential axis observed in Fig. 1 originates from at least two sources. A kinetic contribution, due to the variation of the charge transfer rate with temperature, and a larger thermodynamic contribution (accounting for ca. 60 mV), due to the expected increase of entropy that accompanies the reduction of the hydrated Zn^{2+} ion. To assess this last effect quantitatively, reversible half-wave potentials ($E_{1/2}^r$) were determined by extrapolating the reversible part of the dc wave to ln $[I/(I_{lim} - I)] = 0$, in the ln $[I/(I_{lim} - I)]$ vs E plots. Then, values of the formal potentials (E_f) at different temperatures were computed from $E_f = E_{1/2}^r + (RT/2F)\ln(D_O/D_R)^{1/2}$. Fig. 2b illustrates the variation of E_f with temperature for the four $NaClO_4$ solutions investigated. If changes in thermal liquid junction potentials are neglected [27], then the slopes of the plots in Fig. 2b provide the value of the standard reaction entropy for the reduction of Zn^{2+}:

$$\Delta S^0_{Zn^{2+}/Zn(Hg)} = 2F\frac{dE_f}{dT} = 200 \pm 10 \text{ J mol}^{-1} \text{ K}^{-1} \quad (2)$$

which is independent of the $NaClO_4$ concentration. It should be noted that variation of the Zn^{2+} activity coefficient with temperature accounts for only $\sim 10\%$ of the above value (Appendix A). A recent estimate of absolute ion entropies [28] assigns a value of -361 J mol^{-1} K^{-1} to the hydration entropy of Zn^{2+}. Therefore, the $\Delta S^0_{Zn^{2+}/Zn(Hg)}$ value indicated above may be viewed as the result of a large positive contribution, due to Zn^{2+} dehydration, and a smaller negative contribution (-161 J mol^{-1} K^{-1}), associated with the charge redistribution and amalgamation processes.

Charge transfer rate constants k_f were derived from faradaic impedance measurements. The frequency dependence of the cell admittance was fitted to a Randles equivalent circuit, and charge transfer resistances R_{ct} and Warburg coefficients σ were obtained at each potential. Due to the sluggish charge-transfer kinetics that characterize Zn^{2+} reduction, R_{ct} was often obtained with a higher accuracy than σ, and our results therefore rely mainly on the analysis of the R_{ct} values. To determine k_f from R_{ct} or σ, some functional relationship between k_f and the electrode potential has to be adopted. Similar results were obtained when ln k_f was developed as a power series in terms of electrode potential [4] or, alternatively, when the expected functionality for a two charge transfer steps mechanism was adopted [3]:

$$\frac{1}{k_f} = \frac{1}{k_{f,1}} + \frac{1}{k_{f,2}} = \frac{\exp(\alpha_1^{ap} f\varphi)}{k_{s,1}} + \frac{\exp[(\alpha_2^{ap} + 1)f\varphi]}{k_{s,2}} \quad (3)$$

where $\varphi = (E - E_f)$, $f = F/RT$, α_1^{ap} and α_2^{ap} are apparent transfer coefficients associated with the first and second charge transfer steps, respectively, and $k_{s,1}$ and $k_{s,2}$ are the corresponding rate constants at the formal potential of the overall charge transfer process. Fig. 3 illustrates the adequacy of Eq. (3) to fit the observed behavior of R_{ct}, and it also shows how $\ln k_f$ retains the same dependence on potential upon changing the temperature (Fig. 3b).

Aside from its mechanistic implications, Eq. (3) represents a convenient formalism to summarize the charge transfer kinetics collected at various temperatures and supporting electrolyte compositions. As may be seen in Fig. 4a and b, values close to 0.5 were found for α_1^{ap} and α_2^{ap}, their average values being 0.47 and 0.50, respectively. Both charge transfer coefficients appear to be independent of temperature, within an estimated precision of ± 0.02. It may also be noted that α_2^{ap} is independent of electrolyte concentration, whereas α_1^{ap} displays a small systematic trend with ionic strength, its average value being 0.49 in the presence of 0.5 and 1 M $NaClO_4$, 0.47 in the presence of 2 M $NaClO_4$, and 0.44 in the most concentrated 4 M $NaClO_4$ solution.

The temperature dependence of k_f may be expressed in terms of the experimental real enthalpy of activation, which is defined as [19]:

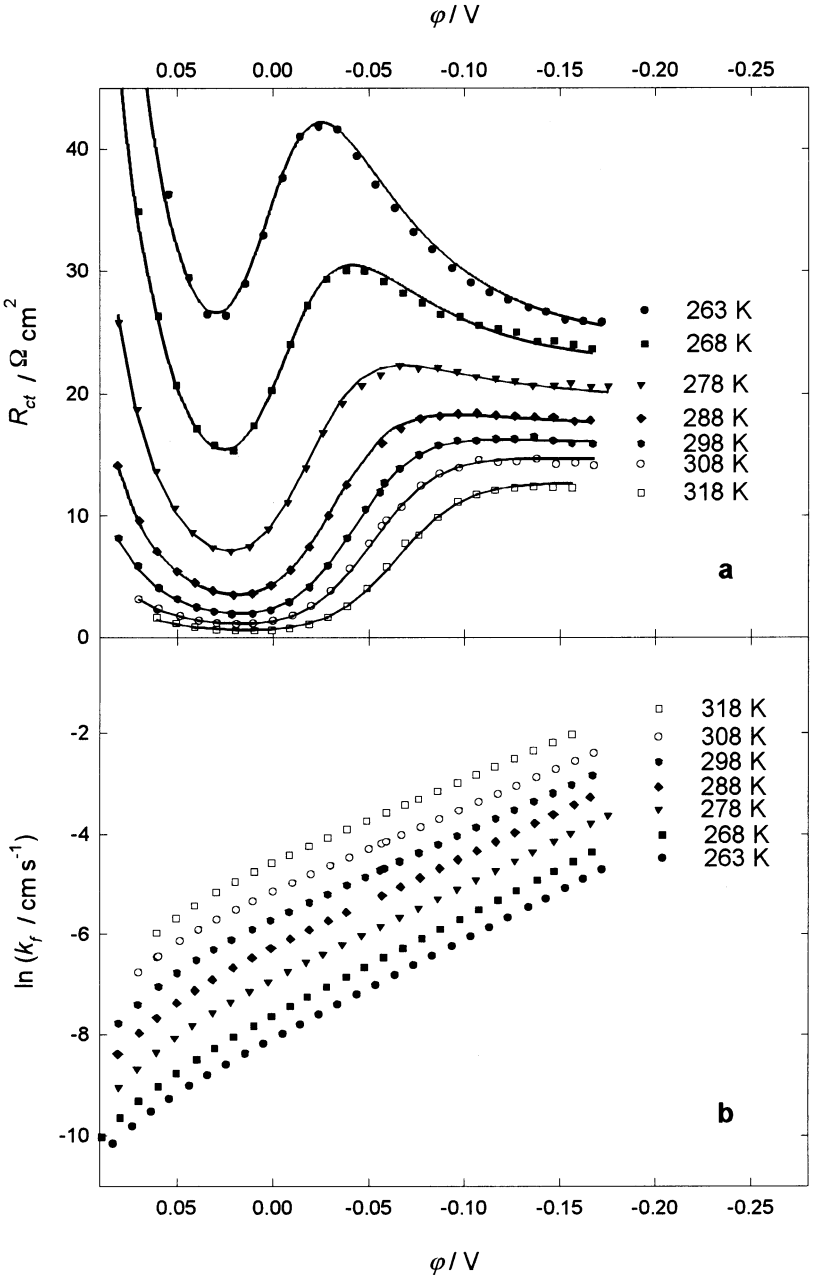

Fig. 3. Variation with temperature of (a) charge transfer resistance (normalized to 20 mM Zn^{2+} concentration), and (b) logarithm of the forward rate constant for Zn^{2+} reduction in the presence of 4 M $NaClO_4$ supporting electrolyte. Temperature is indicated on each curve.

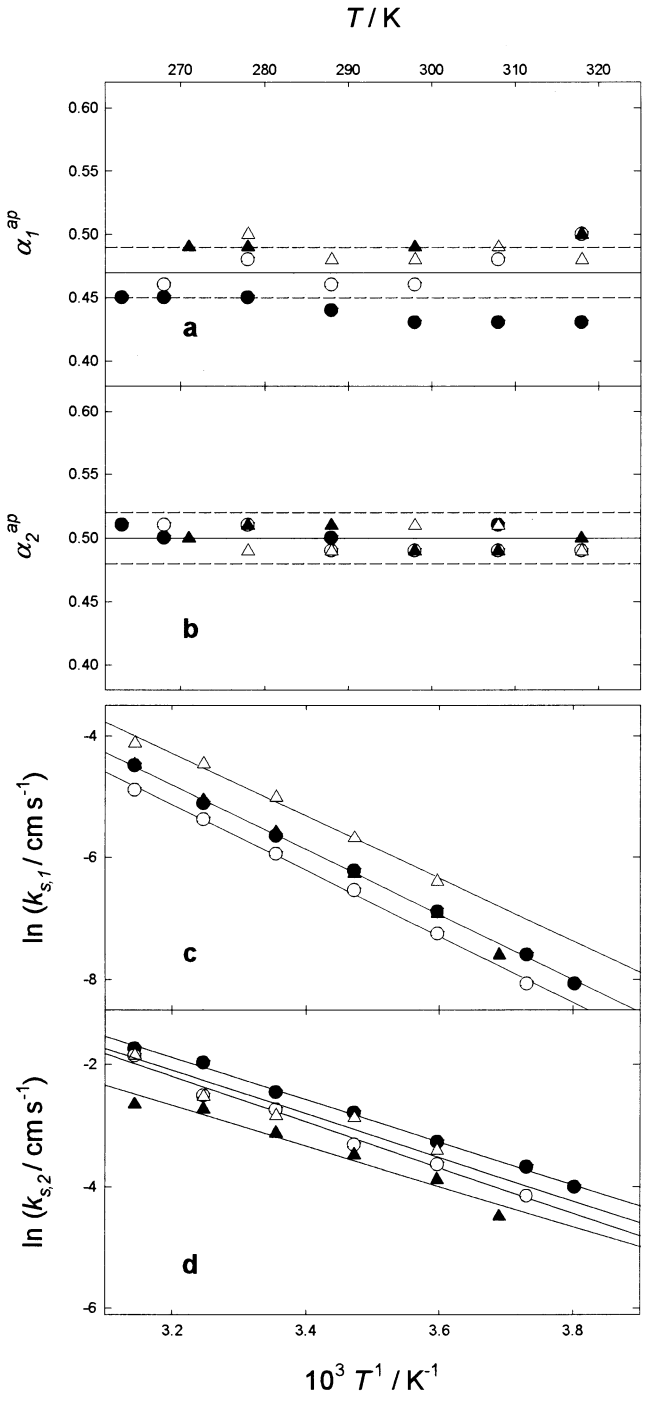

Fig. 4. Dependence of the charge transfer coefficients α_1^{ap} (a) and α_2^{ap} (b) on temperature, and Arrhenius plots of the logarithm of the standard rate constants for the first $\ln k_{s,1}$ (c) and second $\ln k_{s,2}$ (d) charge transfer steps. Solid lines in (a) and (b) correspond to the average values of the charge transfer coefficients, and expected limits of experimental error are indicated with broken lines. Solid lines in (c) and (d) represent least squares fits of experimental data. Symbols correspond to the following sodium perchlorate concentrations: (△) 0.5 M, (▲) 1 M, (○) 2 M and (●) 4 M.

$$\Delta H_{\mathrm{exp}}^{\neq} = -R\left(\frac{\partial \ln k_{\mathrm{f}}}{\partial(1/T)}\right)_{\varphi} \tag{4}$$

Combining Eq. (3) and Eq. (4), it follows that:

$$\begin{aligned}(\Delta H_{\mathrm{exp}}^{\neq})_{\varphi=0} &= -R\left(\frac{\mathrm{d}\ \ln k_{\mathrm{s}}}{\mathrm{d}(1/T)}\right) \\ &= (\Delta H_{\mathrm{exp},1}^{\neq})_{\varphi=0} + (\Delta H_{\mathrm{exp},2}^{\neq})_{\varphi=0} \\ &\quad + R\left(\frac{\mathrm{d}\ \ln(k_{\mathrm{s},1} + k_{\mathrm{s},2})}{\mathrm{d}(1/T)}\right)\end{aligned} \tag{5}$$

where:

$$(\Delta H_{\mathrm{exp},i}^{\neq})_{\varphi=0} = -R\left(\frac{\mathrm{d}\ \ln k_{\mathrm{s},i}}{\mathrm{d}(1/T)}\right)(i = 1, 2) \tag{6}$$

Both $(\Delta H_{\mathrm{exp},1}^{\neq})_{\varphi=0}$ and $(\Delta H_{\mathrm{exp},2}^{\neq})_{\varphi=0}$ were found to be independent of temperature and electrolyte concentration (Fig. 4c and d). The rate constant for the first charge transfer turned out to be more sensitive to temperature changes, and its activation enthalpy $(\Delta H_{\mathrm{exp},1}^{\neq})_{\varphi=0} = 44 \pm 1$ kJ mol^{-1} is significantly higher than the value obtained for the second charge transfer $(\Delta H_{\mathrm{exp},2}^{\neq})_{\varphi=0} = 29 \pm 2$ kJ mol^{-1}. It should be noted also that $(\Delta H_{\mathrm{exp}}^{\neq})_{\varphi=0} \approx (\Delta H_{\mathrm{exp},1}^{\neq})_{\varphi=0}$, since $k_{\mathrm{s},2} \gg k_{\mathrm{s},1}$. This $(\Delta H_{\mathrm{exp}}^{\neq})_{\varphi=0}$ value is in good agreement with previous estimates by Randles and Somerton in 1 M KNO_3 [29] and by Hush and Blackledge in 0.2, 2 and 3 M $NaClO_4$ solutions [30].

Kinetic parameters of electrode reactions are expected to be affected by the interaction of reactants and products with the electrical field of the electrode and with other ions in solution [31,32]. Therefore, it is necessary to correct for these effects before proceeding further with the kinetic analysis.

3.2. Double layer and activity coefficient corrections

Since Zn^{2+} reduction takes place at potentials ca. 0.5 V negative of the potential of zero charge E_{pzc}, we assumed that perchlorate was not specifically adsorbed in the potential range of interest, in agreement with previous findings at 25 °C [33,34]. Then, appropriate interfacial potential profiles can be obtained from the value of the charge density on the metal σ^{M} at each electrode potential, which was determined by integration of the differential capacity C_{d} vs potential curves, starting from their respective E_{pzc} values.

Fig. 5 illustrates, as an example, the temperature dependence of the differential capacity for 1 and 4 M $NaClO_4$ solutions. It may be observed how the hump of the capacity curves decreases and broadens as temperature (or electrolyte concentration) increases. This behavior was also observed in NaF solutions [35], and has been attributed to structural changes of the solvent molecules that populate the inner layer. However, when information available from other electrolytes and solvents is considered, a more detailed picture emerges, where the potential induced solvent reorientation is also related to the nature and surface concentration of

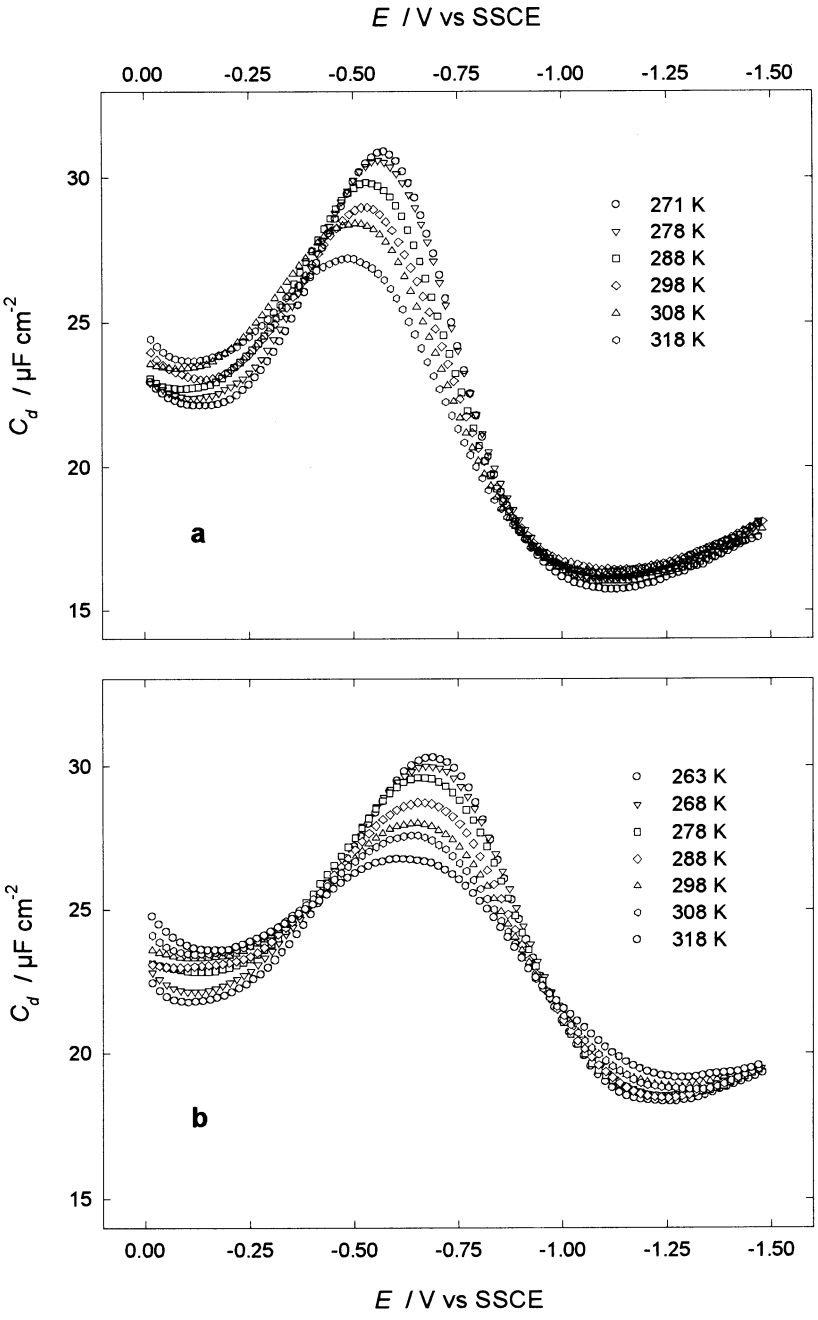

Fig. 5. Variation of the differential capacity of the mercury | aqueous electrolyte interphase with temperature for (a) 1 M and (b) 4 M $NaClO_4$ solutions. Correspondence between symbols and temperature values is indicated on each graph.

specifically adsorbed anions [36]. It should also be noted that the temperature dependence of the differential capacity is rather small in the potential range (from −0.9 to −1.1 V vs SSCE) where Zn^{2+} reduction takes place, presumably due to significant dielectric saturation of solvent molecules in the inner layer.

For a given electrolyte concentration, potentials of zero charge were found to increase linearly with temperature (Fig. 6a), the slopes being 0.67, 0.63, 0.59 and 0.45 mV K^{-1} for the 0.5, 1.0, 2.0 and 4.0 M $NaClO_4$ solutions, respectively. It should be noted that unknown, though apparently small, values of the thermodiffusion liquid junction potentials are included in the measured E_{pzc} values. These results are similar to those reported previously for a series of halides [37], concentrated $NaClO_4$ solutions [25], or potassium sulfate and sodium hydroxide 0.1 M solutions [38]. The increase of the E_{pzc} values with temperature has been explained as due to a decrease of specific adsorption together with a loss of solvent orientation [37]. However, the slopes of the Esin-Markov plots in Fig. 6b can be seen to be nearly independent of temperature, suggesting that solvent

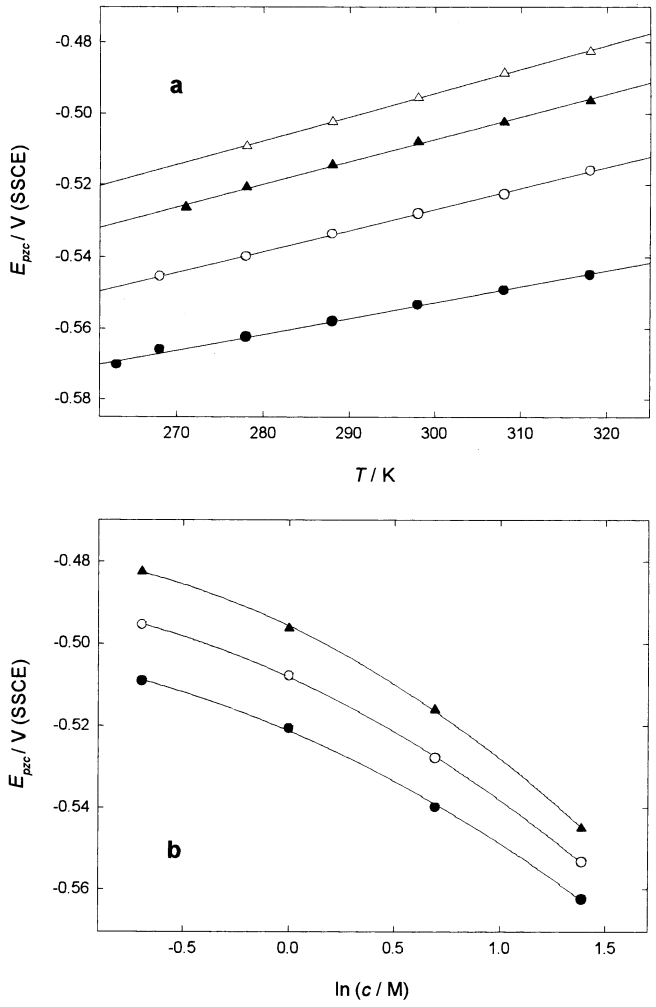

Fig. 6. (a) Variation with temperature of the potential of zero charge measured with respect to an isothermal reference electrode. Sodium perchlorate concentration: (△) 0.5 M, (▲) 1 M, (○) 2 M and (●) 4 M. (b) Variation of the potential of zero charge with the logarithm of $NaClO_4$ concentration at three temperatures: (▲) 318 K, (○) 298 K and (●) 278 K.

reorientation, rather than anion desorption, is the main factor determining the variation of E_{pzc} with temperature in our case. Then, the smaller dE_{pzc}/dT values found in the most concentrated $NaClO_4$ solutions may simply reflect a decrease in the number of freely rotating solvent molecules in the inner layer, due to more extensive ion-solvent interactions in the vicinity of the electrode surface.

In order to correct charge transfer rate constants for double layer effects, it is usually assumed that the activated complex is located at the plane of closest approach of the supporting electrolyte, and the average potential at this plane is computed according to Gouy-Chapman theory (ϕ^{GC}). When this classical procedure is applied to Zn^{2+} reduction in aqueous $NaClO_4$ solutions, a large overcorrection of the double layer effects results [4,20]. Since Zn^{2+} is more strongly solvated than Na^+, the most likely origin of this overcorrection is the non-coincidence of the reaction plane with the plane of closest approach of Na^+ to the electrode. Moreover, the molecular dynamics simulations of Pecina and Schmickler [18] indicate that the less hydrated Zn^+ intermediate approaches the electrode surface more closely than Zn^{2+} does. Therefore, an appropriate double layer correction should recognize the presence of two distinct reaction planes, which do not necessarily coincide with any of the planes of closest approach of the cation and anion of the supporting electrolyte.

A proper account of the Frumkin effect should result in the corrected kinetic parameters being independent of the concentration (and nature) of the electrolyte present in the electrochemical cell. The electrolyte, which includes zinc perchlorate in our case, exerts a twofold influence on the reaction rate, since it determines the potential profile across the double layer and the value of the reactant activity coefficient in solution. Explicit consideration of double layer and activity coefficient effects in Eq. (3) leads to [20]:

$$\frac{\gamma_{Zn^{2+}}\exp(-2f\phi^{rp1})}{k_f} = \frac{\exp[\alpha_1^{cor} f(\varphi - \phi^{rp1})]}{k_{s,1}^{cor}} + \frac{\exp[(1+\alpha_2^{cor})f(\varphi - \phi^{rp1})]}{k_{s,2}^{cor}\exp[(1-\alpha_2^{cor})f(\phi^{rp1} - \phi^{rp2})]} \quad (7)$$

where $\gamma_{Zn^{2+}}$ is the activity coefficient of Zn^{2+} in solution, $k_{s,i}^{cor}$ and α_i^{cor} are the corrected standard rate constant and transfer coefficient, respectively, and ϕ^{rp1} and ϕ^{rp2} are the average potentials at the planes where the first and second charge transfer take place, respectively. Eq. (7) has been derived under the assumption that activity coefficients of intermediate species at both reaction planes are independent of potential and electrolyte concentration.

It has been shown [20] that correction for double layer effects on the rate of Zn^{2+} reduction can be achieved by using the unequal distances of closest approach (UDCA) theory [39–41], which accounts explicitly for the individual distances of closest approach of all ions in solution, including the reactant and the Zn^+ intermediate.

To compute ϕ^{rp1} and ϕ^{rp2} from UDCA theory, it is necessary to specify the dielectric properties of the interphase. We shall adopt the same distances of closest approach (a_i) and relative permittivity (ε_i) values that were employed previously [20]. Therefore, we shall assume that $\varepsilon_1 = 6$ for the first layer of water molecules in direct contact with the electrode surface, $\varepsilon_2 = 33$ up to a distance of 0.59 nm from the electrode, a region which is populated only by cations according to the distances of closest approach indicated below, and we shall take ε_3 in

the diffuse layer equal to the bulk solvent permittivity, which will be allowed to vary with temperature as described in the literature [42]. The distances of closest approach of Na^+ ($a_{Na^+} = 0.31$ nm) and ClO_4^- ($a_{ClO_4^-} = 0.59$ nm) were obtained from electrocapillary measurements [34], and those of Zn^{2+} ($a_{Zn^{2+}} = 0.39$ nm) and H^+ ($a_{H^+} = 0.25$ nm) were derived from an empirical correlation between hydrated radii and distances of closest approach. For the unstable Zn^+ intermediate two alternatives have been envisaged, either it is assumed that Zn^+ remains fully hydrated and it has the same solvated radius as Na^+ (then $a_{Zn^+} = 0.31$ nm), or that it becomes contact-adsorbed on the electrode surface (then $a_{Zn^+} = 0.09$ nm [18]).

The ratio of the UDCA estimate for the potential at the first reaction plane ϕ^{rp1} and the value derived from Gouy-Chapman theory for the potential at the oHp ϕ^{GC} is depicted in Fig. 7a as a function of overpotential, for two $NaClO_4$ concentrations and at two temperatures. It may be observed that $|\phi^{rp1}|$ remains smaller than $|\phi^{GC}|$ in the potential range of interest, due to electrostatic screening of the reaction plane by the supporting electrolyte cations. Upon increasing electrolyte concentration, the cationic charge within the anion-free layer overcompensates the electronic charge on the electrode, leading to small positive values of ϕ^{rp1} for $\varphi \geqslant 0.1$ V in the 4 M $NaClO_4$ solution. The difference between the UDCA potentials at the two reaction planes, $\phi^{rp1} - \phi^{rp2}$, is strongly dependent on their relative locations, and increases with increasing separation. Fig. 7b illustrates its dependence on the $\varphi - \phi^{rp1}$ potential scale (which is used below to construct Frumkin corrected plots) for the extreme $a_{Zn^{2+}} = 0.39$ nm and $a_{Zn^+} = 0.09$ nm values. Note that, upon varying the $NaClO_4$ concentration from 0.5 to 4 M, changes of $\sim$ 50 mV in $\phi^{rp1} - \phi^{rp2}$ are predicted for positive overpotential values, where the second term in Eq. (7) is expected to provide a significant contribution to the observed reaction rate.

When cathodic rate constants are corrected for the potential drop between solution and the plane of closest approach of Zn^{2+}, as well as for changes in its activity coefficient (Appendix A), Frumkin corrected plots are obtained which are independent of $NaClO_4$ concentration within experimental error (Fig. 8). Therefore, a unique $k_f^{cor} = f(\varphi - \phi^{rp1})$ functional relationship between k_f^{cor} and $\varphi - \phi^{rp1}$ can be defined at each temperature. This result indicates that actual $\phi^{rp1} - \phi^{rp2}$ values are smaller than those computed in Fig. 7a for $a_{Zn^{2+}} = 0.39$ nm and $a_{Zn^+} = 0.09$ nm, and it suggests that the distance between the two reaction planes is smaller than 0.3 nm. As temperature is increased, the loss of linearity in the Frumkin corrected plots occurs at lower overpotentials, in agreement with a higher value of the activation enthalpy for the first charge transfer step at the formal potential of the overall Zn^{2+} reduction.

Corrected charge transfer coefficients were found to be independent of temperature (Fig. 9a), with average values of 0.47 for α_1^{cor} and 0.50 for α_2^{cor}, though the absolute accuracy of the α_2^{cor} values is probably not better than 0.1, despite their low degree of scatter in Fig. 9a, since they are determined over a rather narrow potential range. Corrected activation enthalpies are somewhat higher than the previous uncorrected values, thus $(\Delta H^{\neq}_{cor,1})_{\varphi - \phi^{rp1} = 0} = 49$ kJ mol^{-1}, $(\Delta H^{\neq}_{cor,2})_{\varphi - \phi^{rp1} = 0} = 31$ kJ mol^{-1} for $a_{Zn^+} = 0.31$ or 0.39 nm and $(\Delta H^{\neq}_{cor,2})_{\varphi - \phi^{rp1} = 0} = 38$ kJ mol-1 for $a_{Zn^+} = 0.09$ nm (Fig. 9b). The intercepts of the Arrhenius plots in Fig. 9b give estimates of the frequency factors, which are larger for the first ($A_{cor,1} = 7 \times 10^5$ cm s^{-1}) than for the second ($A_{cor,2} = 1.5 \times 10^4$ cm s^{-1}) charge transfer steps. It should be noted that, upon deriving the above activation enthalpy values, we have neglected any temperature dependence of the pre-exponential factors, whose contribution to the activation enthalpy is expected to be small anyway [32].

4. Discussion

Amalgam forming reactions consist of, at least, three processes: charge transfer, loss of the cationic solvation sheath and amalgamation. The interplay between these processes leads typically to non linear Tafel plots, which indicate a change in the rate determining step upon varying the potential. In contrast with simple electron exchange reactions, where reactant displacement through the double layer plays only a secondary role, transfer of an ion under the action of the interfacial electric field must now be considered as a relevant contribution to the reaction coordinate, and may by itself constitute the rate determining step of the overall process [12].

In the case of Zn^{2+} reduction, the variation of the logarithm of the forward rate constant with potential, depicted in Fig. 3b and Fig. 8, indicates the presence of two consecutive charge transfer steps, whose nature may be associated with either two successive electron transfers, or a combination of ion transfer and adsorption steps [17]. The high value of the Zn^{2+} hydration enthalpy [28] makes a simultaneous loss of solvation and transfer of the doubly charged cation across the double layer rather unlikely. A smaller energetic price is to be paid if Zn^{2+} is first reduced to Zn^+ and, subsequently, Zn^+ is either reduced or transferred to an adsorption site on the mercury surface [13].

An analysis of the activation parameters corresponding to the first charge transfer step in terms of current electron transfer theories is hampered by the inaccessibility of its standard potential ($E_{f,1}$). If it is assumed that $E_{f,1} \approx E_f$ for the overall process (which also implies that $E_{f,2} \approx E_f$), then the previous $(\Delta H^{\neq}_{cor,1})_{\varphi - \phi^{rp1} = 0}$ estimate

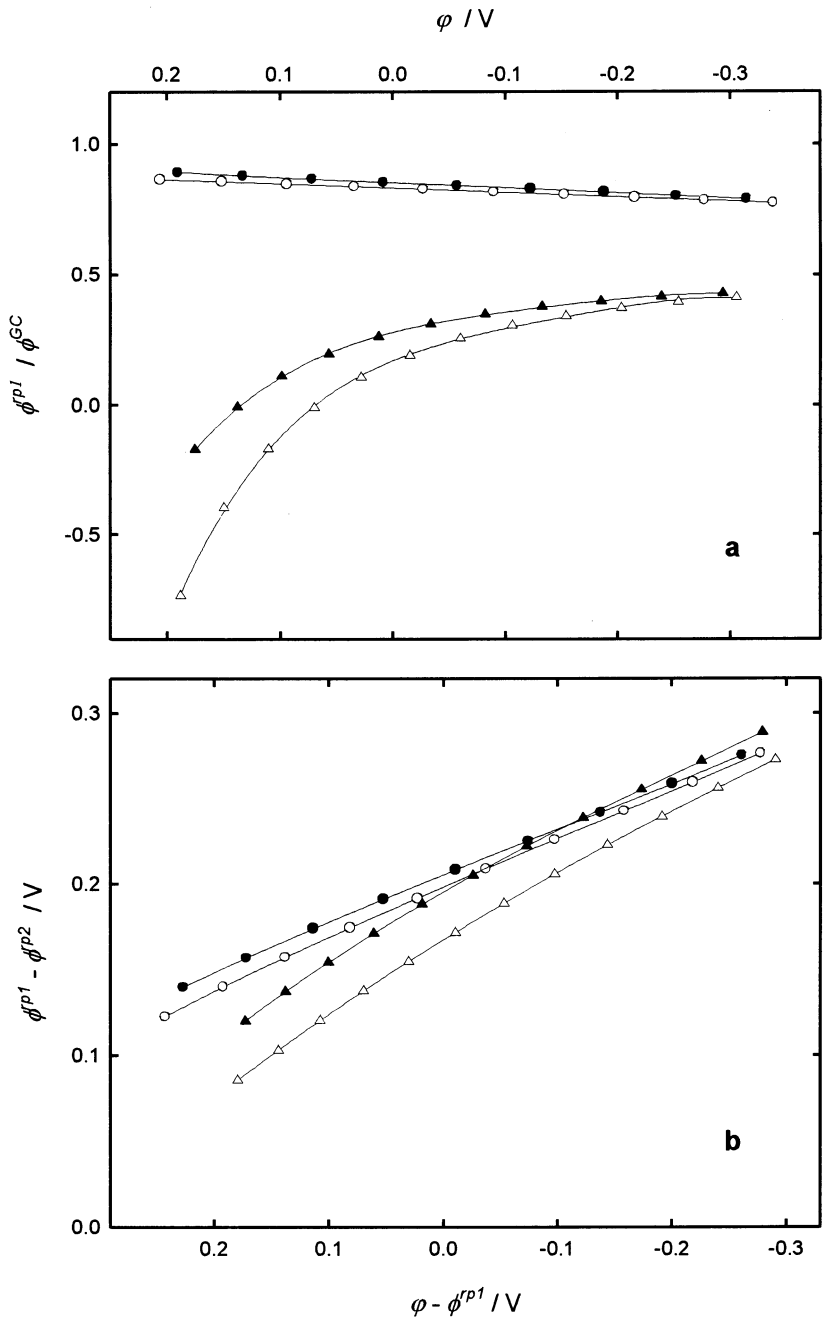

Fig. 7. (a) Potential dependence of the ratio between the UDCA potential at the first reaction plane and the Gouy-Chapman potential at the oHp, as a function of $NaClO_4$ concentration: (○, ●) 0.5 M, (△, ▲) 4 M, and temperature: (○, △) 318 K, (●, ▲) 278 K. (b) Difference between the UDCA potentials at the two reaction planes as a function of the ϕ^{rp1} corrected overpotential, assuming that $a_{Zn^{2+}} = 0.39$ nm and $a_{Zn^{+}} = 0.09$ nm. Symbols as in (a).

can be shown to agree with the expected value for a dielectric charging activation process leading to electron transfer [43]. Additionally, $A_{cor,1}$ lies within the 10^5–10^6 cm s^{-1} range predicted by the encounter pre-equilibrium model for electron transfer (upon neglecting any contribution from the activation entropy and assuming that the transmission coefficient $\kappa \approx 1$ [44]), and a value of α_1^{cor} close to 0.5 also seems to support the electron transfer hypothesis, implying a symmetric activation barrier.

On the basis of a molecular dynamics study of the solvent influence on the electrochemical transfer of divalent ions, Pecina and Schmickler [18] have suggested that the first electron transfer step in the Zn^{2+} reduction mechanism is preceded by an ion transfer step, which involves the loss of one water molecule from the first

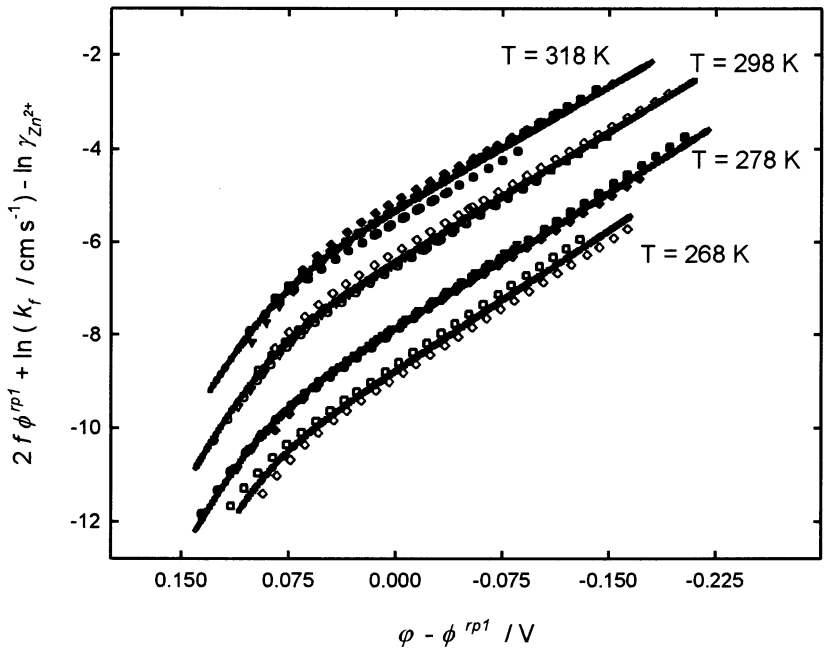

Fig. 8. Corrected Frumkin plots for Zn^{2+} reduction at different temperatures. The ϕ^{rp1} potential was estimated from UDCA theory, assuming that the first charge transfer step takes place at 0.39 nm from the electrode surface. Activity coefficients of Zn^{2+} in the solution bulk $\gamma_{Zn^{2+}}$ were computed as described in Appendix A. Symbols indicate different sodium perchlorate concentrations: (○, ●) 0.5 M, (▽, ▼) 1 M, (□, ■) 2 M, (◇, ◆) 4 M. Open and filled symbols are alternated for successive temperatures, for the sake of clarity. Solid lines are fits of corrected data to Eq. (7) at each temperature.

solvation shell. Thus, the activation of Zn^{2+} to reach a configuration appropriate for the acceptance of one electron would imply a displacement of its center of charge by ca. 0.08 nm from its plane of closest approach and a partial dehydration. To account for a combined ion transfer and electron transfer step, an extra factor $\exp(\alpha_1^{cor} f(\phi^{rp1} - \phi^{rp2}))$ should be included in the first term on the right hand side of Eq. (7), which results in only a slight modification of the $k_{s,1}^{cor}$ values for such a small displacement. Interestingly, there is a good coincidence between the molecular dynamics estimate of the Gibbs energy required to reach the activated configuration of Zn^{2+} and the $(\Delta H_{cor,1}^{\neq})_{\varphi - \phi^{rp1} = 0}$ value determined previously.

The Frumkin corrected activation enthalpy for the first charge transfer step may be considered as the true value associated with this elementary step, except perhaps for a possible contribution from changes in the ion-solvent interaction energy. However, the activation enthalpy for the second charge transfer step should be regarded as an apparent value, containing the (unknown) enthalpic change corresponding to the first charge transfer step. In any case, the difference of ca. 20 kJ mol^{-1} between these two activation enthalpies suggests that the intermediate Zn^{+} may be more stable than previous estimates indicate [13], and helps to rationalize the value of α_1^{cor} in terms of a more symmetrical barrier for the first charge transfer step. The pre-exponential factor $A_{cor,2}$ turned out to be twenty times smaller than $A_{cor,1}$, and its value would be even smaller if a correction for the increase in entropy, that presumably accompanies the first charge transfer step, were to be made. Since there are no obvious reasons to expect a decrease in the electronic interaction between mercury and Zn^{+}, as compared to the interaction with Zn^{2+}, a more plausible origin of the disparity between the pre-exponential factors is a change in the nature of the elementary step. A value of $\alpha_2^{cor} \approx 0.5$ would still be compatible with an ion transfer step [17], but it should take place over a short distance ($\leqslant 0.1$ nm), due to the lack of sensitivity of $k_{s,2}^{cor}$ towards changes in the $\phi^{rp1} - \phi^{rp2}$ value brought about by the supporting electrolyte.

The theoretical calculations of Pecina and Schmickler [18] also indicate that a lower true activation barrier ($\sim$ 30 kJ mol^{-1}) would be expected for the second charge transfer step, as compared to the first charge transfer step, when the former consists of a Zn^{+} displacement to an adsorption site on the electrode surface. Ion transfer steps involve a disruption of the solvent structure in the vicinity of the electrode surface, and their activation energy and charge transfer coefficient have been predicted to decrease as the temperature increases [21,45], due to a weakening of the interfacial water structure. From this point of view, our results indicate that neither of the two rate determining steps can be identified as an

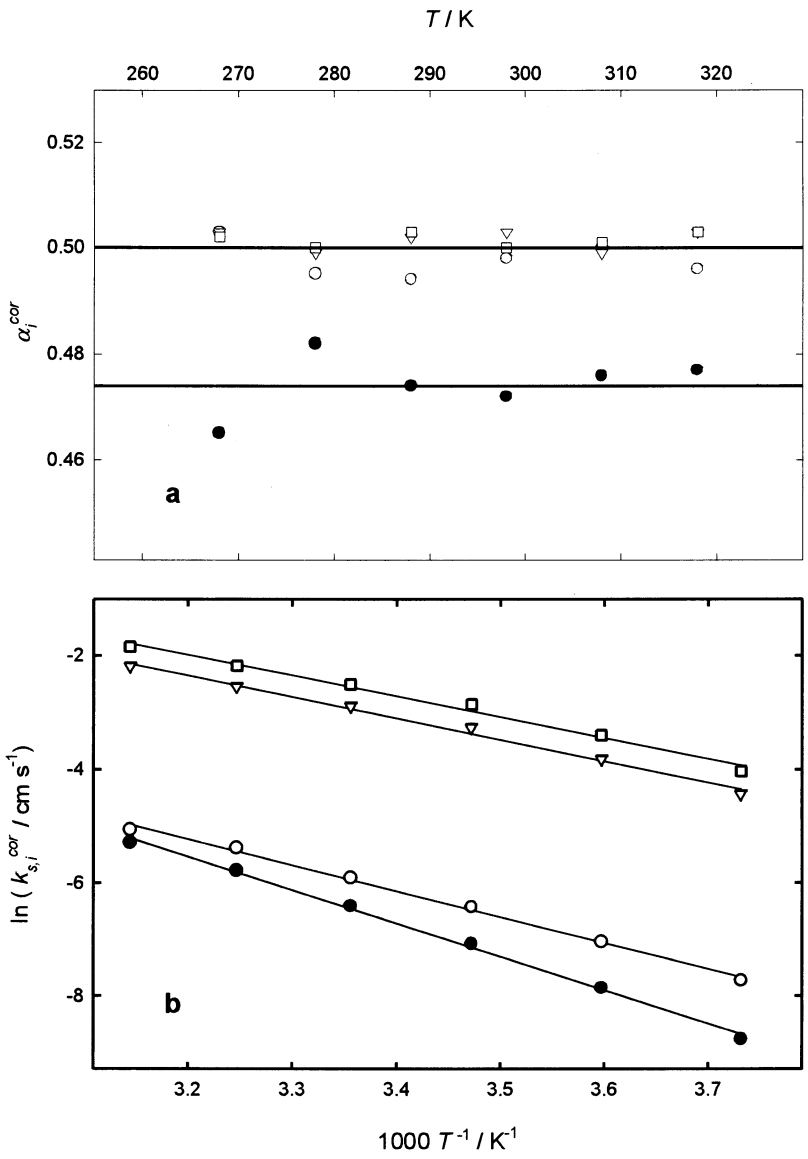

Fig. 9. (a) Dependence of the Frumkin corrected charge transfer coefficients α_1^{cor} (filled symbols) and α_2^{cor} (open symbols) on temperature, and (b) Arrhenius plots for the first (filled symbols) and second (open symbols) charge transfer steps. Solid lines in (a) correspond to average values of the charge transfer coefficients. Solid lines in (b) represent least squares fits to the data. Kinetic parameters for the second charge transfer step were computed for: $a_{Zn^{2+}} = 0.09$ nm (○), $a_{Zn^{2+}} = 0.31$ nm (▽) and $a_{Zn^{2+}} = 0.39$ nm (□).

ion transfer step. However, it should be kept in mind that Zn^{2+} reduction takes place at potentials far negative with respect to the potential of zero charge, where dielectric saturation effects may render the interfacial water structure rather insensitive to moderate changes in temperature.

Summarizing, the values obtained for the activation parameters seem to be compatible with the overall physical picture that emerges from Pecina and Schmickler's simulations, in as much as the interfacial water structure is mainly determined by the electrical field, and remains essentially unaltered by the changes in temperature that we have explored in this work.

5. Conclusions

We have shown that the variations of the logarithm of the forward rate constant of Zn^{2+} reduction with potential and temperature can be described quantitatively by a reaction mechanism consisting of two consecutive charge transfer steps, whose activation enthalpies and charge transfer coefficients are independent of temperature in the 263–318 K range. Corrections of double layer effects, according to UDCA theory, and of changes in the Zn^{2+} activity coefficient, according to MSA theory, lead to a single functional relationship between corrected rate constants and over-

potential at each temperature, independent of the supporting electrolyte concentration. This result suggests that the activated complexes of the two charge transfer steps are separated by a distance not exceeding 0.1 nm. The values of the true activation enthalpy, pre-exponential factor and charge transfer coefficient for the first charge transfer step agree with the expected values for a simple electron exchange process, provided its formal potential value is assumed to be similar to that corresponding to the overall process. Comparison of the activation enthalpies for the first and second charge transfer steps indicates that the increase in enthalpy associated with the reduction of Zn^{2+} to Zn^{+} is lower than ~ 20 kJ mol^{-1}.

Acknowledgements

This work has been supported by the Dirección General de Investigación Científica y Tecnológica (DGICYT) under Grant PB098-1123. Helpful comments by Dr W.H. Mulder are also gratefully acknowledged.

Appendix A

The procedure for computing trace activity coefficients of Zn^{2+} ($\gamma_{Zn^{2+}}$) in the presence of an excess of $NaClO_4$ supporting electrolyte is described in this appendix. Activity coefficients were derived from MSA theory applied to the extended primitive model [46], in which ion radius r_i^{bulk} and solution permittivity ε^{bulk} were allowed to vary with electrolyte concentration according to:

$$r_i^{bulk} = (r_i^{bulk})_{c\to 0} + \beta c \tag{A1}$$

$$\varepsilon^{bulk} = \frac{(\varepsilon)_{c\to 0}}{1 + \alpha c} \tag{A2}$$

where c is the molar electrolyte concentration, $(r_i^{bulk})_{c\to 0}$ and $(\varepsilon)_{c\to 0}$ are the ionic radius and the solvent permittivity at infinite dilution, respectively, and α and β are empirical parameters used to fit the concentration dependence of r_i^{bulk} and ε^{bulk}.

The temperature dependence's of $(r_i^{bulk})_{c\to 0}$, β and α are described by [47]:

$$(r_i^{bulk})_{c\to 0} = (r_i^{bulk})_{c\to 0}^{298} + r_1\tau \tag{A3}$$

$$\beta = b_0 + b_1\tau + b_2\tau^2 \tag{A4}$$

$$\alpha = a_0 + a_1\tau + a_2\tau^2 \tag{A5}$$

where $\tau = T - 298$ K.

Activity coefficients of $NaClO_4$ and $Zn(ClO_4)_2$ at temperatures different from 298 K have not been found in the literature, so they have been estimated using the following strategy. First, activity coefficients for these electrolytes at 298 K [48] have been used to obtain the values of a_0 and b_0 in Eqs. (A4) and (A5). Values of $(r_i^{bulk})_{c\to 0}^{298}$ and r_1 for Na^{+} have been taken from Ref. [47], and those for Zn^{2+} were derived from the temperature dependence of ZnI_2 activity coefficients [49]. Values of a_1, a_2, b_1 and b_2 for $NaClO_4$ have been taken as the average of those tabulated for NaCl and $HClO_4$ in Ref.

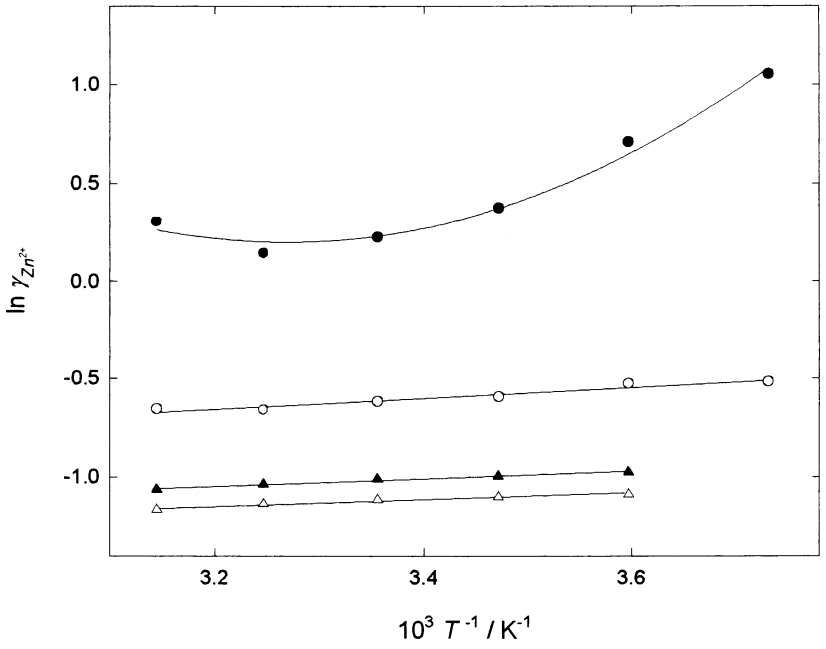

Fig. A1. Arrhenius plot of the logarithm of the Zn^{2+} trace activity coefficient, in the presence of: (△) 0.5 M, (▲) 1 M, (○) 2 M and (●) 4 M $NaClO_4$ solutions.

[47], whereas a_1, a_2, b_1 and b_2 for $Zn(ClO_4)_2$ have been assumed to be the same as for ZnI_2.

The validity of these approximations has been tested by reproducing the relative apparent molal enthalpy (Φ_L) of these electrolytes, which is defined as [50]:

$$\Phi_L = \nu RT^2 \left[\left(\frac{\partial \Psi}{\partial T} \right)_{P,m} - \left(\frac{\partial \ln \gamma_{\pm}}{\partial T} \right)_{P,m} \right] \quad \text{(A6)}$$

where ν is the electrolyte stoichiometric number, Ψ the osmotic coefficient, $\gamma_{\pm}$ the mean activity coefficient, and the other symbols have their usual meaning.

The Φ_L values computed from MSA theory have been compared with experimental values tabulated for $NaClO_4$ [51] and $Zn(ClO_4)_2$ [52], and a satisfactory agreement (within ca. 10%) between calculated and experimental values was found in the concentration range of interest. Next, trace activity coefficients of Zn^{2+} in the presence of an excess of supporting electrolyte were computed as described in the literature [46,47], and are plotted in Fig. A1. The slopes of these plots contribute typically ~ 3 kJ mol^{-1} to the activation enthalpy, which increases up to ~ 10 kJ mol^{-1} in the case of the most concentrated $NaClO_4$ solution at low temperatures.

References

[1] T. Erdey-Gruz, Kinetics of Electrode Processes, Adam Hilger, London, 1972 (chapter 4).
[2] V.V. Losev, in: B.E. Conway, J.O'M. Bockris (Eds.), Modern Aspects of Electrochemistry, vol. 7, Plenum Press, New York, 1972, p. 314.
[3] C.P.M. Bongenaar, A.G. Remijnse, M. Sluyters-Rehbach, J.H. Sluyters, J. Electroanal. Chem. 111 (1980) 139.
[4] R. Andreu, M. Sluyters-Rehbach, A.G. Remijnse, J.H. Sluyters, J. Electroanal. Chem. 134 (1982) 101.
[5] J. Struijs, M. Sluyters-Rehbach, J.H. Sluyters, J. Electroanal. Chem. 171 (1984) 177.
[6] M. Saakes, M. Sluyters-Rehbach, J.H. Sluyters, J. Electroanal. Chem. 259 (1989) 265.
[7] A.S. Baranski, W.R. Fawcett, J. Chem. Soc. Faraday Trans. 1 76 (1980) 1962.
[8] A.S. Baranski, W.R. Fawcett, J. Chem. Soc. Faraday Trans. 1 78 (1982) 1279.
[9] W.R. Fawcett, J.S. Jaworski, J. Chem. Soc. Faraday Trans. 1 78 (1982) 1971.
[10] W.R. Fawcett, S. Yee, J. Electroanal. Chem. 306 (1991) 271.
[11] M. Sluyters-Rehbach, J.H. Sluyters, Electrochim. Acta 33 (1988) 983.
[12] W.R. Fawcett, J. Phys. Chem. 93 (1989) 2675.
[13] M.T.M. Koper, W. Schmickler, J. Electroanal. Chem. 450 (1998) 83.
[14] G. Salié, Z. Phys. Chem. Leipzig 244 (1970) 1.
[15] T. Hurlen, E. Eriksrud, J. Electroanal. Chem. 45 (1973) 405.
[16] F. van der Pol, M. Sluyters-Rehbach, J.H. Sluyters, J. Electroanal. Chem. 58 (1975) 177.
[17] W.R. Fawcett, J. Electroanal. Chem. 302 (1991) 13.
[18] O. Pecina, W. Schmickler, Chem. Phys. 252 (2000) 349.
[19] W.R. Fawcett, S. Yee, J. Electroanal. Chem. 366 (1994) 219.
[20] G. López-Pérez, R. Andreu, D. González-Arjona, M. Molero, J.J. Calvente, J. Phys. Chem. A 105 (2001) 9156.
[21] O. Pecina, W. Schmickler, E. Spohr, J. Electroanal. Chem. 405 (1996) 239.
[22] D. González-Arjona, G. López-Pérez, E. Roldán, J.D. Mozo, Electroanalysis 12 (2000) 1143.
[23] R. Andreu, D. González-Arjona, M. Domínguez, M. Molero, E. Roldán, Electroanalysis 3 (1991) 377.
[24] D.C. Grahame, E.M. Coffin, J.I. Cummings, M.A. Poth, J. Am. Chem. Soc. 74 (1952) 137.
[25] S. Marczak, P.W. Wrona, Z. Galus, J. Electroanal. Chem. 471 (1999) 62.
[26] Z. Galus, Pure Appl. Chem. 56 (1984) 635.
[27] E.L. Yee, R.J. Cave, K.L. Guyer, P.D. Tyma, M.J. Weaver, J. Am. Chem. Soc. 101 (1979) 1131.
[28] W.R. Fawcett, J. Phys. Chem. B 103 (1999) 11181.
[29] J.E.B. Randles, K.W. Somerton, Trans. Faraday Soc. 48 (1952) 951.
[30] N.S. Hush, J. Blackledge, J. Electroanal. Chem. 5 (1963) 420.
[31] W.R. Fawcett, Can. J. Chem. 59 (1981) 1844.
[32] W.R. Fawcett, Z. Kováčová, J. Electroanal. Chem. 292 (1990) 9.
[33] B.B. Damaskin, A.N. Frumkin, V.F. Ivanov, N.I. Melekhova, V.F. Khonina, Elektrokhimiya 4 (1968) 1336.
[34] G. López-Pérez, D. González-Arjona, M. Molero, R. Andreu, Langmuir 15 (1999) 4892.
[35] D.C. Grahame, J. Am. Chem. Soc. 79 (1957) 2093.
[36] R. Parsons, Rev. Pure Appl. Chem. 18 (1968) 91.
[37] W. Paik, T.N. Andersen, H. Eyring, J. Phys. Chem. 71 (1967) 1891.
[38] J.E.B. Randles, K.S. Whiteley, Trans. Faraday Soc. 52 (1956) 1509.
[39] K. Joshi, R. Parsons, Electrochim. Acta 4 (1961) 129.
[40] J.P. Valleau, G.M. Torrie, J. Chem. Phys. 76 (1982) 4623.
[41] R. Andreu, M. Molero, J.J. Calvente, J. Carbajo, J. Electroanal. Chem. 58 (1993) 49.
[42] K.N. Marsh (Ed.), IUPAC. Recommended Reference Material for the Realization of Physicochemical Properties, Blackwell Scientific Publications, Oxford, 1987.
[43] N.S. Hush, J. Chem. Phys. 28 (1958) 962.
[44] J.T. Hupp, M.J. Weaver, J. Electroanal. Chem. 152 (1958) 1.
[45] O. Pecina, W. Schmickler, E. Spohr, J. Electroanal. Chem. 394 (1995) 29.
[46] J.P. Simonin, J. Phys. Chem. B 101 (1997) 4313.
[47] G. López-Pérez, D. González-Arjona, M. Molero, J. Electroanal. Chem. 480 (2000) 9.
[48] R.A. Robinson, R.H. Stokes, Electrolyte Solutions, second ed., Butterworths, London, 1970.
[49] R.G. Bates, J. Am. Chem. Soc. 60 (1938) 2983.
[50] F.J. Millero, in: R.M. Pytkowicz (Ed.), Activity Coefficients in Electrolyte Solutions, vol. II, CRC Press, Boca Raton, 1980.
[51] V.B. Parker, Thermal Properties of Aqueous Uni-univalent Electrolytes, National Standard Reference Data Series, Unites States Department of Commerce, 1965, p. 55.
[52] R.L. Berg, C.E. Vanderzee, J. Chem. Thermodynamics 7 (1975) 219.